Distribution of the wavefunction inside chaotic partially open systems

P. Šeba
Nuclear Physics Institute, Czech Academy of Sciences, 250 68 Řež, Czech Republic
Pedagogical University, Hradec Kralove, Czech Republic

F. Haake
Fachbereich Physik, Universität-GH Essen, Essen, Germany

M. Kuś
Center for Theoretical Physics, Polish Academy of Sciences, Warsaw, Poland

M. Barth, U. Kuhl, H.-J. Stöckmann
Fachbereich Physik, Universität Marburg, D-35032 Marburg, Germany
(February 5, 2008)

arXiv:chao-dyn/9705009v1 6 May 1997

We demonstrate both theoretically and experimentally that the distribution of the wavefunction inside a partially open chaotic timereversal symmetric system displays significant deviations from the Porter Thomas distribution. We give arguments which show that this distribution resembles the distribution which is expected to be found in closed chaotic systems with broken time reversal symmetry.

PACS numbers: 05.45.+b

It is now generally accepted that in the ballistic regime the scattering on boundaries of a chaotic mesoscopic quantum dot leads to irregular scattering phenomena which are measurable during the transport of electrons through the dot. Usually it is assumed that ideal leads are attached to the quantum dot and the conductance G is evaluated using Landauer formula relating the conductance with the corresponding S matrix

$$S = \begin{pmatrix} r & t \\ t' & r' \end{pmatrix} \tag{1}$$

where r, t are the reflection and transmission matrices. In terms of S matrix the conductance reads

$$G = \frac{e^2}{h} \mathrm{Tr}\left(tt^+\right). \tag{2}$$

Essentially the same mechanism can be applied also to the transmission of microwaves through irregularly shaped cavities. In this case G denotes the total transmission probability (of course in this case the factor e^2/h has to be omitted!). The microwave experiments have the advantage that all components of the scattering matrix are obtained directly from the measurement, and that scattering geometries can be easily varied in a controlled manner. Therefore the results to be derived below will be tested using results from microwave cavities containing randomly distributed scatterers.

Investigating conductance fluctuations the standard argument assumes that the S matrix belongs to some random matrix ensemble (usually the circular orthogonal (COE) or unitary (CUE) ensemble). There is, however, also another aspect of the statistical properties of the S matrix elements which relates the S matrix elements with the internal wavefunction.

The S matrix maps the incoming waves into the outgoing ones. Therefore knowing S and the structure of the incoming part of the wave inside the leads one can easily evaluate the value of the wavefunction at the points where the leads couple to the resonator. Since we assume an ideal coupling of the leads on the quantum dot the wavefunction is smooth at the coupling points. This means that the internal wavefunction at *the coupling points* equals the wavefunction inside the leads. Therefore from a knowledge of the statistical properties of the S matrix we can obtain information about the properties of the internal wavefunction.

It is the aim of this letter to develop the above heuristic arguments and to show to what extent the transport through the dot changes the structure of the wavefunction. Let us start with some remarks: the important role of the internal wavefunction during the transport through weakly open systems (resonance transport) has been used in [1,2] to investigate the statistical properties of the conductance. In these papers the applied strategy was however just opposite to what we try to do here: the conductance distribution was obtained *assuming* that the internal wavefunction is chaotic and has a Porter-Thomas distribution. On the other hand there are also works which followed the same strategy and used the measured S matrix to determine the internal wavefunction, see for instance [3,4]. It

has to be stressed, however, that in all these cases theinvestigations are restricted to the resonance scattering regime and theinfluence of the transport on the structure of the internal wavefunction hasbeen neglected.

To begin the investigation let us first construct a simple Hamiltonian which leads to the S matrix being usually used as a starting point for the description of transmission fluctuations. Starting with the description of the leads we assume that they support M open channels and are described by one-dimensional Hamiltonians

$$H_l = -\frac{d^2}{dx^2} + \lambda_l \ , \ l = 1, .., M. \tag{3}$$

Here λ_l is the threshold energy of the l-th channel and x denotes the coordinate along it. Combining these operators into a Hamiltonian H_{ex} for the "external" part of the system we get

$$H_{ex} = -\mathbf{1}\frac{d^2}{dx^2} + \Lambda, \tag{4}$$

where Λ is a diagonal matrix describing the threshold energies of the channels,

$$\Lambda = diag\left(\lambda_1, \lambda_2, .., \lambda_M\right), \tag{5}$$

and 1 is the the $M \times M$ identity matrix. The resonator is described by a Hermitian matrix H_{in} of size $N \times N$, where N corresponds to the number of eigenenergies taken into account, with N much larger than the number of open channels, $N \gg M$. The matrix H_{in} is assumed to belong to the Gaussian orthogonal / unitary Ensemble (GOE/GUE) for chaotic cavities (see e.g. [5] for these concepts). To describe the scattering we couple the resonator and leads by defining the Hamiltonian $H$of the whole system as

$$H\begin{pmatrix} u \\ u_{in} \end{pmatrix} = \begin{pmatrix} H_{ex}u \\ H_{in}u_{in} + Au'(0) \end{pmatrix}, \tag{6}$$

where $u = (u_1, \ldots, u_M)$ stands for the wavefunction inside the leads and u_{in} describes the wavefunction within the resonator. $u'(0)$ denotes the vector of derivatives of the wave functions inside the leads taken at the points of contacts with the resonator (i.e. at zero of each lead coordinate). A is the $N \times M$ coupling matrix. Later on we will specify the coupling matrix A by assuming that the coupling has a local character (point contacts). This assumption is justified whenever the diameter of the junction is smaller than a typical wavelength inside the resonator.

Let us now return to the Hamiltonian H. In the form it is given by (6) the operator is not symmetric. To make it symmetric an additional boundary condition is needed:

$$A^\dagger u_{in} = -u(0). \tag{7}$$

It is not difficult to show, that under these condition the Hamiltonian H is a self-adjoint operator – for the proof see [6].

Before proceeding further we have to specify the structure of the internal Hamiltonian matrix H_{in}. On the most general level we assume only that this matrix belongs to the Gaussian orthogonal (unitary) ensemble. Less abstractly it will be however helpful to construct this matrix using the knowledge of the specific properties of the resonator in consideration. To specify H_{in} we use the Hamiltonian H_{res} of the resonator (usually a two dimensional Laplace operator with Dirichlet boundary conditions). Let E_n and $f_n(\vec{r})$ be the eigenvalues and eigenfunctions of H_{res},

$$H_{res}f_n(\vec{r}) = E_n f_n(\vec{r}). \tag{8}$$

Using these solutions we define a finite dimensional internal Hamiltonian acting on the space spanned by the first N eigenstates of H_{res},

$$H_{in} = \sum_{n=1}^{N} E_n f_n f_n^\dagger. \tag{9}$$

The coupling operator A maps the vector $u'(0)$ into a certain function belonging to the N dimensional internal space. Let $u(x) = (u_1(x), u_2(x), \ldots, u_M(x))$ denote the components of the wave function in the attached open channels. Applying the matrix A to the incoming vector we get

$$\begin{aligned} Au'(0) &= \sum_{m=1}^{M}\sum_{n=1}^{N} u'_m(0)A_{nm}f_n \\ &= \alpha_1 d_1^N(\vec{r})u'_1(0) + \alpha_2 d_2^N(\vec{r})u'_2(0) + \ldots + \alpha_M d_M^N(\vec{r})u'_M(0), \end{aligned} \tag{10}$$

where $\alpha_l d_l^N = \sum_{n=1}^N A_{nl} f_l$; $\alpha_1, \ldots, \alpha_M$ are the coupling constants of the individual channels and $d_l^N,\ l = 1, \ldots, M$ are functions spanned by the vectors $f_n;\ n = 1, \ldots, N$. In the experiment the channels are locally coupled to the resonator at points $\vec{r}_1, \ldots, \vec{r}_M$. Here $\vec{r}_1, \ldots, \vec{r}_M$ refer to the coordinate system chosen inside the resonator and correspond to the zero points of the coordinates inside the leads. In order to mimic this local coupling we choose the functions $d_l^N(\vec{r}),\ l = 1, \ldots, M$ in a special way which ensures their convergence to $\delta(\vec{r} - \vec{r}_l)$ for $N \to \infty$, namely

$$d_l^N(\vec{r}) = \sum_{i=1}^{N} f_i(\vec{r}_l) f_i(\vec{r}). \tag{11}$$

In the sense of generalized functions one has $\lim_{N\to\infty} d_l^N(\vec{r}) = \delta(\vec{r} - \vec{r}_l)$.

At this point few remarks are necessary: First of all it has to be stressed that now the coupling matrix A is completely determined by M constants $\alpha_1, \ldots, \alpha_M$. The boundary condition (7) takes now the form $< \alpha_l d_l^N, u_{in} >= -u_l(0)$, where $<,>$ denotes the scalar product in the N-dimensional Hilbert space of functions inside the resonator. In the limit $N \to \infty$ this boundary conditions are thus given by the formula

$$\alpha_l u_{in}(\vec{r}_l) = -u_l(0), \tag{12}$$

which relates the internal wavefunction at the coupling point to the wavefunction inside the corresponding lead. If we assume that the contact is ideal, i.e. that the wavefunctions match smoothly at the contact, $u_{in}(\vec{r}_l) = u_l(0)$, we obtain $\alpha_l = -1$ for all l. The components of the coupling matrix A are then given by

$$A_{lm} = -f_l(\vec{r}_m). \tag{13}$$

Equation (12) becomes a starting point for a further consideration of the statistical properties of the internal wavefunction.

Since the information about the structure of the internal wavefunction is hidden in the scattering data we have first to evaluate the corresponding S matrix. Following [6] we solve the equation $HU = EU$ for a scattering energy E. The eigenfunction

$$U(E) = \begin{pmatrix} u(E,x) \\ u_{in} \end{pmatrix} \tag{14}$$

solves the equations

$$\begin{pmatrix} -\frac{d^2}{dx^2} u(E,x) + \Lambda u(E,x) \\ H_{in} u_{in}(E) + A u'(E,0) \end{pmatrix} = E \begin{pmatrix} u(E,x) \\ u_{in} \end{pmatrix}. \tag{15}$$

For energies $E > \lambda_j,\ j = 1, \ldots, M$, the scattering solution inside the leads can be presented in the form

$$u(E,x) = \frac{e^{-i\sqrt{E-\Lambda}x}}{\sqrt[4]{E-\Lambda}} \mathcal{A}_{inc} - \frac{e^{i\sqrt{E-\Lambda}x}}{\sqrt[4]{E-\Lambda}} \mathcal{A}_{out}, \tag{16}$$

where $\mathcal{A}_{inc}, \mathcal{A}_{out}$ are the amplitudes of the incoming and outgoing wave, respectively. For all $E > max\{\lambda_j\}$ every solution is bounded and the scattering matrix $S(E)$ can easily be defined. The normalization used in (16) ensures that the S matrix relates the amplitudes of the incoming and outgoing waves as

$$\mathcal{A}_{out} = S(E) \mathcal{A}_{inc}. \tag{17}$$

The scattering matrix can be calculated substituting (16) into (15) and applying the boundary condition (7) which leads to

$$S(E) = \frac{i + W^\dagger (E - H_{in})^{-1} W}{i - W^\dagger (E - H_{in})^{-1} W}, \tag{18}$$

where $W = AQ^{-1}$ and $Q \equiv Q(E)$ denotes the $M \times M$ matrix $Q(E) = (E - \Lambda)^{-\frac{1}{4}}$. This S matrix can be rewritten as [6]

$$S(E) = 1 - 2iW^\dagger \frac{1}{E - H_{eff}} W, \tag{19}$$

where $H_{eff} = H_{in} + iWW^{\dagger}$ stands for the effective, nonhermitian Hamiltonian. The assumption on the point character of the contact leads in the limit $N \to \infty$ to $H_{eff} = H_{res} + i\sum_{n=1}^{M} \alpha_n^2 \sqrt{E-\lambda_n}\ \delta(\vec{r}-\vec{r}_n)$. Effective Hamiltonians of this type has been used previously on a heuristic level in [1] for the description of conductance fluctuations in quantum dots. In the present case, however, the coupling of the imaginary effective potential depends on energy (frequency) of the incident wave. This fact has been observed experimentally in [7].

For the value of the external component $u(E,x)$ at the coupling points we get from (10)

$$u(E,0) = Q(1-S)\mathcal{A}_{inc}; \tag{20}$$

and finally from (12) a relation between the S matrix and the internal function:

$$\begin{pmatrix} u_{in}(\vec{r}_1) \\ u_{in}(\vec{r}_2) \\ \vdots \\ u_{in}(\vec{r}_M) \end{pmatrix} = Q(S-1)\mathcal{A}_{inc}. \tag{21}$$

The relation (21) is valid not only for the case of a resonant scattering but also in situations with many overlapping resonances. This can be understood when the formula is compared with previous results, where a relation between the resonance wavefunction and the S matrix was obtained for the case of one *isolated* resonance [1,2,4]. The relation (21) gives us the possibility to look for the structure of the internal wavefunction in situations where the S matrix belongs to certain ensembles of random unitary matrices.

In a typical experiment the wave is fed into the resonator through one of the attached channels - say through the first one - and the wavefunction is measured either by measuring the reflection in the entrance lead or the transmission to an exit lead. This means that $\mathcal{A}_{inc} = (1,0,..,0)$ and

$$u_{in}(\vec{r}_k) = \frac{1}{(E-\lambda_k)^{1/4}}\,(S_{1k} - \delta_{1k}) \tag{22}$$

with $k=1$ in the reflection case and $k>1$ in the transmission case. Assuming λ_k to be constant (i.e. not varying from sample to sample) we obtain finally that the statistics of $u_{in}(\vec{r}_k)$ coincides with the statistics of the S matrix elements S_{1k}.

It is widely accepted that the structure of the S matrix of a chaotic system with time reversal symmetry is described by a generalized circular ensemble (so called Poisson kernel) introduced by Gaudin and Mello [8], see also [9]. The structure of this ensemble is fully determined by the mean value $< S >$ of the S matrix. The mean value describes the "quality" of the contact. It is related to the coupling matrix W by [10]

$$< S_{ll} >= \frac{1-\gamma_l}{1+\gamma_l} \tag{23}$$

with γ_l given by

$$\sum_{n=1}^{N} W_{nl}W_{mn} = \delta_{lm}\gamma_m. \tag{24}$$

Note that the orthogonality relation (24) follows from (13) and is satisfied whenever the distance between the coupling points exceeds the typical wavelength in the scattering problem. In the case of ideal coupling we have $< S >= 0$ and the ensemble coincides with the Circular Orthogonal Ensemble of Dyson. The relation between the Poisson kernel and S matrices of the form (18) is described in [11].

The statistics of the corresponding S matrix elements S_{kl} was evaluated in [12]. It was shown that for sufficiently large M the S-matrix elements can be regarded as statistically independent. Moreover the real and imaginary part of S_{kl} are independent Gaussian distributed variables.

Let us first consider a measurement of the transmission between leads 1 and 2. Denoting $S_{12} = X + iY$ and following [12] we obtain

$$P(S_{12}) = \frac{\sqrt{ab}}{\pi} e^{-aX^2} e^{-bY^2} \tag{25}$$

with a, b given by

$$\begin{array}{c} a = \frac{1+<S11><S22>}{(1-<S_{11}>^2)(1-<S_{22}>^2)} \\ b = \frac{1-<S11><S22>}{(1-<S_{11}>^2)(1-<S_{22}>^2)} \end{array} \tag{26}$$

and $< S_{11} >, < S_{22} >$ being the mean values of the corresponding matrix elements (they are assumed to be real for simplicity). Finally using (22) we obtain for the distribution of the modulus of the normalized internal wavefunction at point $\vec{r}_2$ [13]

$$P\left(|u_{in}|^2\right) = Z \exp\left(-Z^2|u_{in}|^2\right) I_0\left(Z\sqrt{Z^2-1}|u_{in}|^2\right) \tag{27}$$

with

$$Z = \frac{1}{\sqrt{1- < S_{11} >^2 < S_{22} >^2}}. \tag{28}$$

A similar relation holds also for the reflection measurement. The internal wavefunction is studied using the matrix element S_{11} which measures the direct reflection of the wave into the incoming channel. For the distribution of $S_{11} = X + iY$ one has [12]:

$$P(S_{11}) = \frac{\sqrt{ab}}{\pi} e^{-a(X-<X>)^2} e^{-bY^2} \tag{29}$$

with the coefficients a, b given by

$$\begin{array}{c} a = \frac{1+<S11>^2}{(1-<S_{11}>^2)^2} \\ b = \frac{1}{1-<S_{11}>^2} \end{array} \tag{30}$$

and with $< S_{11} >=< X >$ denoting the mean of the S matrix element. Using that we get for the distribution of the normalized internal wavefunction

$$< u_{in} >= 1- < S_{11} > \tag{31}$$

and for the distribution of $\tilde{u}_{in} = u_{in} - < u_{in} >$

$$P\left(|\tilde{u}_{in}|^2\right) = Z \exp\left(-Z^2|\tilde{u}_{in}|^2\right) I_0\left(Z\sqrt{Z^2-1}|\tilde{u}_{in}|^2\right) \tag{32}$$

with Z equal to

$$Z = \frac{1}{\sqrt{1- < S_{11} >^4}}. \tag{33}$$

In the COE case with $< S >= 0$ (ideal coupling of channels) both distributions (27) and (32) lead to Poissonian distribution:

$$P(\left(|u_{in}|^2\right) = \exp\left(-|u_{in}|^2\right). \tag{34}$$

In the other extreme case of very weakly coupled channels for which we have $< S_{11} > \approx < S_{22} > \approx \pm 1$ and hence $Z \to \infty$, which reduces (27) to the Porter-Thomas-distribution

$$P\left(|u_{in}|^2\right) = \frac{1}{\sqrt{2\pi|u_{in}|^2}} \exp\left(-\frac{|u_{in}|^2}{2}\right). \tag{35}$$

The same holds also for the distribution (32) with $< S_{11} > \approx \pm 1$.

It is worth stressing that in the COE case the distribution of the internal wavefunction coincides with the distribution of eigenvectors of an GUE ensemble, i.e. with a case of fully broken time reversal symmetry.

For smaller number of channels the distribution of the S-matrix elements does not factorize and the distribution of the internal wavefunction cannot be found explicitly. Nevertheless it becomes clear that it depends strongly on the number of open channels. For instance in the case of two ideally coupled channels (COE case) we obtain from [14]

$$P\left(|u_{in}|^2\right) = \frac{1}{2\sqrt{2\pi|u_{in}|^2}}. \tag{36}$$

Microwave billiards are especially well suited to test the predictions on distributions of the S-matrix elements (seeEqs. (25) and (29)) and of transmission and reflectionprobabilities (see Eqs. (27) and (32)). Allquantities entering into these expressions are directly available from theexperiment. It is of special importance that there are only two parameters,namely the averages $< S_{11} >$ and $< S_{22} >$. As these quantities, too, canbe measured, there is no free adjustable parameter in the theory.

The measurements were performed in a rectangular microwave resonator with 10 to 17 randomly distributed scatterers; fig. 1 shows a typical arrangement. The number of scatterers should be sufficient to block most of the bouncing ball modes in order to make the system chaotic; on the other hand the mean distance should be at least of the order of the typical wavelength. The measuring technique was described earlier [15,4]. A vector network analyzer, model 360B, Wiltron company, was used supplying real and imaginary part of all components of the S matrix.

To study the transport through the resonator 16 antennae (thin copper wires of diameter 0.2 mm) were put into the resonator. The antennae act as single scattering channels as their diameter is small compared to the wavelength in the total frequency range. Only two antennae were really used for reflection and transmission measurements. Through the antenna 1 microwaves are coupled to the resonator and reflection (S_{11}) is measured. The transmission (S_{12}) is measured with the help of the antenna 2 . All other antennae not used are closed by 50 Ω loads and act as drains for the microwaves.

In Fig. 2 parts of a typical measured S_{11}-spectrum are shown. The qualitative difference between the non-overlapping regime at lower frequencies (a) and the overlapping regime at higher frequencies (b) is immediately evident. For the case of non-overlapping resonances we performed about 600 measurements with different positions of ten scatterers from 2 to 4 GHz with a resolution of 1 MHz. In the region of well separated resonances one can derive from the billiard equivalent of the Breit-Wigner formula a relation between $|u_{in}|^2$ and the measured S_{11} at the maximum of the resonances,

$$|u_{in}|^2 \propto \Gamma(1 - \mathrm{Re}(S_{11})), \tag{37}$$

where Γ is the width of the resonance [4]. We fitted the single resonances in the real part of S_{11} with a Lorentzian and extracted height and width of them to obtain $|u_{in}|^2$. In total we obtained a sample of more than 12000 values for $|u_{in}|^2$. The histogram of these values is shown in Fig. 3 and compared to the theoretical curves for GOE and GUE and the distribution (32) using $Z \approx 1.17$, calculated from the experimentally obtained $< |u_{in}|^2 > \approx 0.72$. The experimental distribution fits very well to the theoretical one. It should be noted that no parameter had to be fitted to obtain this accordance.

At higher frequencies where single resonances are no longer well resolved we can take the total spectrum for the determination of the S-parameters. The calibration poses a problem. By application of standard procedures the influence of cables, connectors etc. is efficiently calibrated away. The influence of the antenna wire itself, however, cannot be removed by the calibration and results in a long range variation of baseline and phase over several GHz. Apart from some regimes, which were excluded from the further analysis, the drift of the phase could be corrected away by a polynomial background subtraction. It was not possible, however, to discriminate between phase drifts from the antenna and real phase shifts by the billiard. Therefore the determination of the phase of S_{11} is necessarily erroneous. This can be seen in Fig. 4a,b where the distributions of $\mathrm{Re}(S_{11} - < S_{11} >)$ (a) and of $\mathrm{Im}(S_{11})$ (b) are plotted. The error in the phase determination is responsible for the clear deviation of the distribution of $\mathrm{Re}(S_{11} - < S_{11} >)$ from a Gaussian. For $\mathrm{Im}(S_{11})$, on the other hand, exactly the expected Gaussian behavior is found though here of course, too, the phase determination is incorrect. But as the average of $\mathrm{Im}(S_{11})$ vanishes in contrast to that of $\mathrm{Re}(S_{11})$, an error in the phase determination is not able to disturb the Gaussian behaviour. It should be noted that errors in the phase do influence only the distribution of $\mathrm{Re}(S_{11} - < S_{11} >)$, for all other distributions discussed here this phase is not of relevance.

In Fig. 5 the histograms obtained from the measured spectra for the distribution of the internal wavefunction $|u_{in}|^2$ for (a) S_{11} (reflection measurement) and (b) S_{12} (transmission measurement) in the region of overlapping resonances are shown. The results are compared with the theoretical predictions (32) and (27) with the parameter $Z \approx 1.06$ calculated from the mean value $< S_{11} >$. As we did not measure S_{22} we assumed $< S_{11} > = < S_{22} >$ to calculate Z from Eq. (28). Since the geometries of the antennae are identical, this assumption seems to be plausible. In Fig. 4c,d we show the distributions of $\mathrm{Re}(S_{12})$ (c) and $\mathrm{Im}(S_{12})$ (d). Again the Gaussian shapes are found in accordance with the theory.

The experiments have shown that the ansatz of random unitary matrices by Pereyra and Mello [12] for the scattering matrix can perfectly account for the observed distribution of S-matrix elements found in our microwave billiard (apart from one point where imperfections in the calibration make the comparison impossible). The change in the Z parameter from $Z = 1.17$ in the case of separated resonances to $Z = 1.06$ in the case of overlapping ones shows further that the presence of the 14 not used antennae closed by 50 Ω transforms the system from the GOE to, essentially, the GUE behaviour. In the region of overlapping resonances we found transmission and reflection behaviour as being

already essentially a GUE-like (see Fig. 5). In other words: the presence of the drains in the form of closed antennae transforms the standing waves of the original billiard, more or less completely, into running waves propagating from the entrance antenna to the different exit ports.

ACKNOWLEDGMENTS

This research has been partially supported by the Foundation for Theoretical Physics in Slemeno, Czech Republic and by the Deutsche Forschungsgemeinschaft via the SFB 185 Nichtlineare Dynamik. M. K. acknowledges the support from Polish KBN Grant 2 P03B 093 09.

---

[1] V. Prigodin, K. Efetov, and S. Iida, Phys. Rev. Lett. **71**, 1230 (1993).
[2] Y. Alhassid, J. Hormuzidar, and N. Whelan, to be published (cond-mat/9609115).
[3] H. Alt *et al.*, Phys. Rev. Lett. **74**, 62 (1995).
[4] J. Stein, H.-J. Stöckmann, and U. Stoffregen, Phys. Rev. Lett. **75**, 53 (1995).
[5] F. Haake, *Quantum Signatures of Chaos* (Springer-Verlag, Berlin, 1991).
[6] S. Albeverio *et al.*, J. Math. Phys. **37**, 4888 (1996).
[7] F. Haake *et al.*, Phys. Rev. A **44**, R6161 (1991).
[8] M. Gaudin and P. Mello, J. Phys. G **7**, 1085 (1981).
[9] P. Mello, P. Pereyra, and T. Seligman, Ann. Phys. (NY) **161**, 254 (1985).
[10] J. Verbaarschot, H. Weidenmüller, and M. Zirnbauer, Phys. Rep. **129**, 367 (1985).
[11] P. Brouwer, Phys. Rev. B **51**, 16878 (1995).
[12] P. Pereyra and P. Mello, J. Phys. A **16**, 237 (1983).
[13] E. Kanzieper and V. Freilikher, Phys. Rev. B **54**, 8737 (1996).
[14] H. Baranger and P. Mello, Phys. Rev. Lett. **73**, 142 (1994).
[15] H.-J. Stöckmann and J. Stein, Phys. Rev. Lett. **64**, 2215 (1990).

FIG. 1. Rectangular billiard (45 cm $*$ 20 cm, height 0.8 cm) with 13 to 17 movable scatterers of diameter 2 cm positioned at random on a 18$*$8-grid. There are 16 fixed antennas (copper wires of diameter 0.2 mm) connected to the billiard at randomly chosen points with a minimum distance of 2.5 cm.

FIG. 2. Parts of a typical S_{11} spectrum after calibrating away the effects of cables and connectors. At lower frequencies the resonances are sharply separated whereas at higher frequencies they overlap.

FIG. 3. Histogram of the $|u_{in}|^2$-values at low frequencies (non overlapping regime) in a semilogarithmic plot. The dashed and dotted lines correspond to Poisson distribution ($Z = 1$, GUE) and Porter-Thomas distribution ($Z \to \infty$, GOE), respectively. The solid line depicts the distribution (32) with the parameter $Z \approx 1.17$ calculated from $< |u_{in}|^2 >$.

FIG. 4. The distributions of real and imaginary parts of $S_{11} - < S_{11} >$ (a,b) and S_{12} (c,d). All distributions are normalized to have the variance equal to one. The solid lines correspond to the expected Gaussian behaviour.

FIG. 5. Histograms of $|u_{in}|^2$ for (a) reflection (S_{11}) and (b) transmission (S_{12}) in a semilogarithmic plot. The dashed and dotted lines correspond to Poisson distribution ($Z = 1$, GUE) and Porter-Thomas distribution ($Z \to \infty$, GOE), respectively. The solid line gives the distribution (32) with the parameter $Z \approx 1.06$ calculated from $< S_{11} >$.

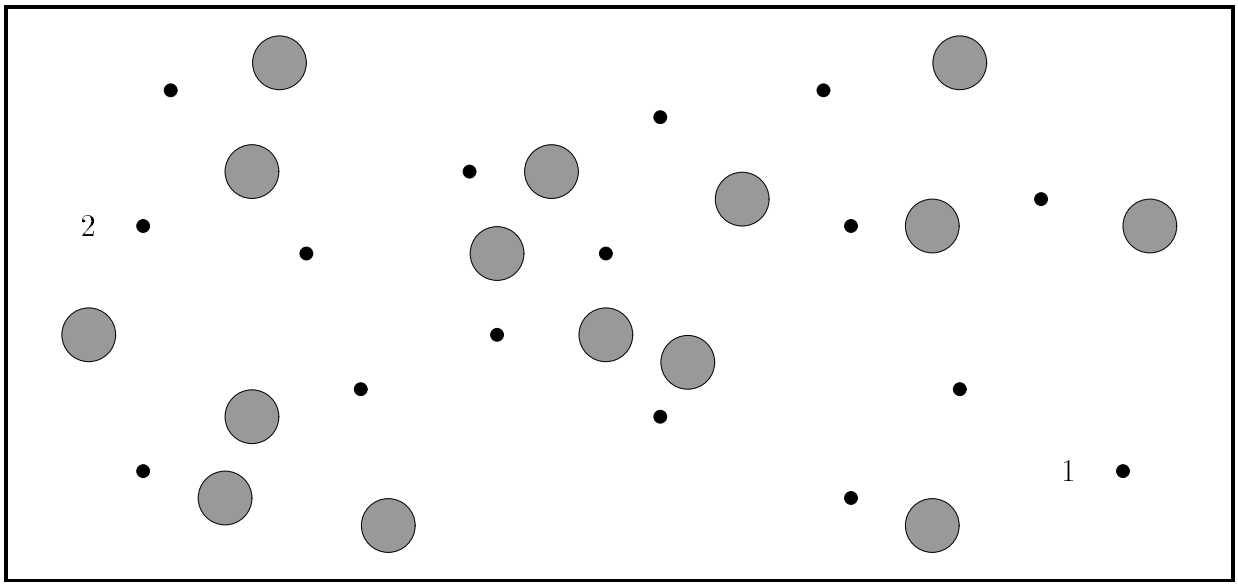

Fig. 1

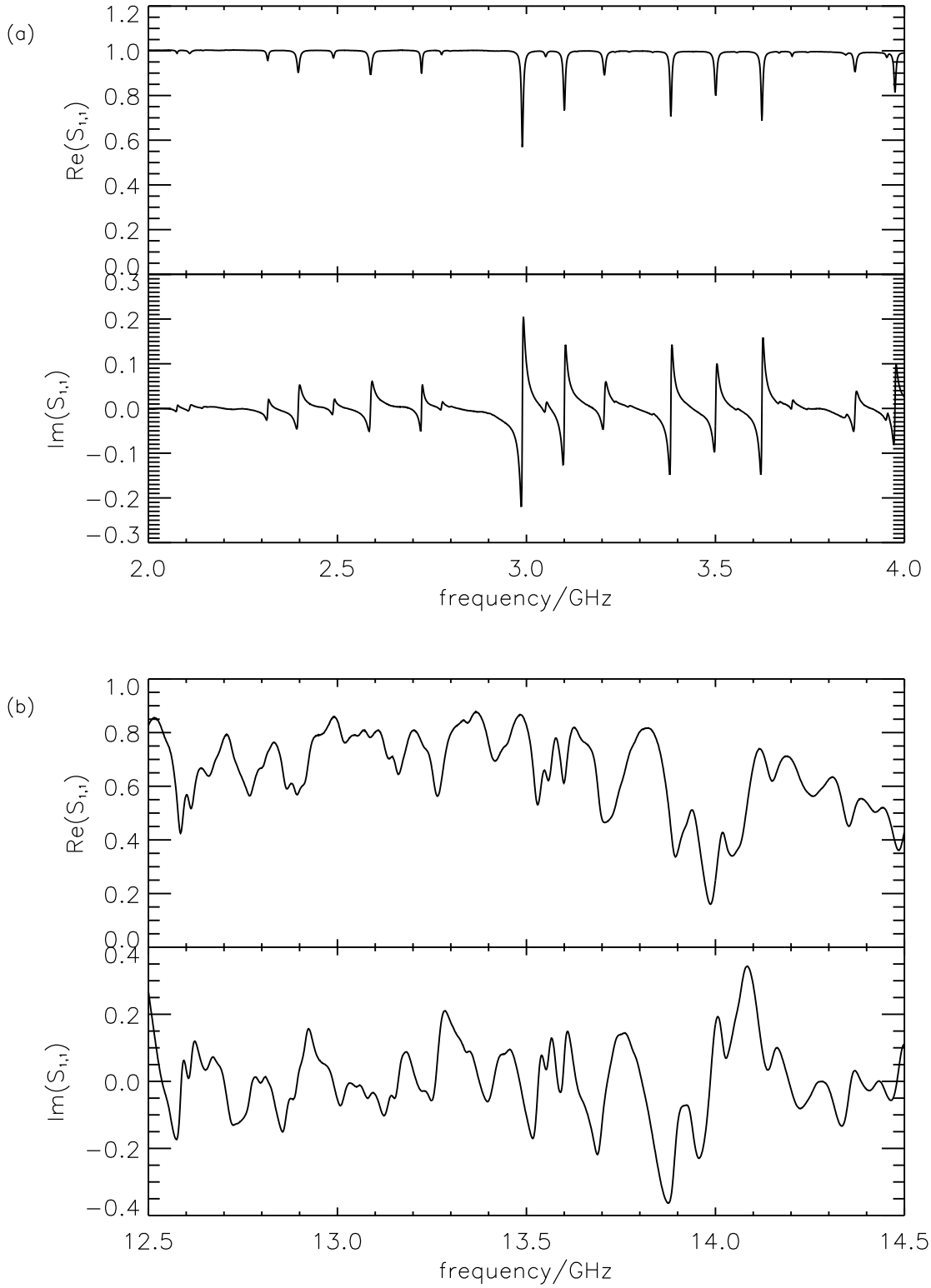

Fig. 2

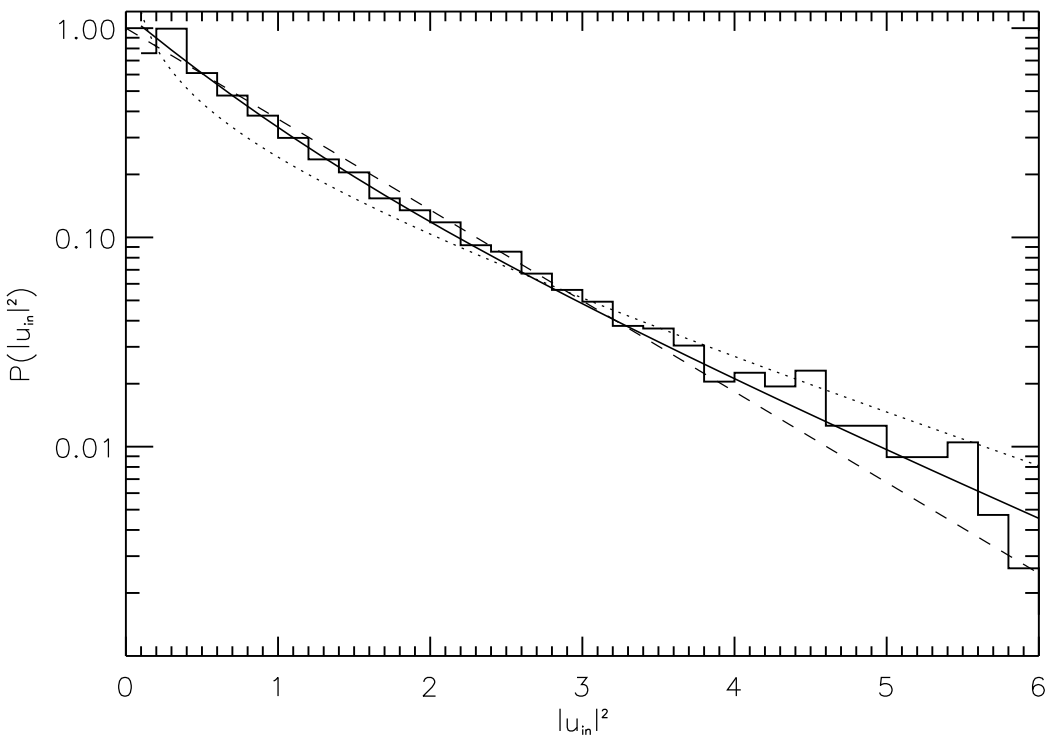

Fig. 3

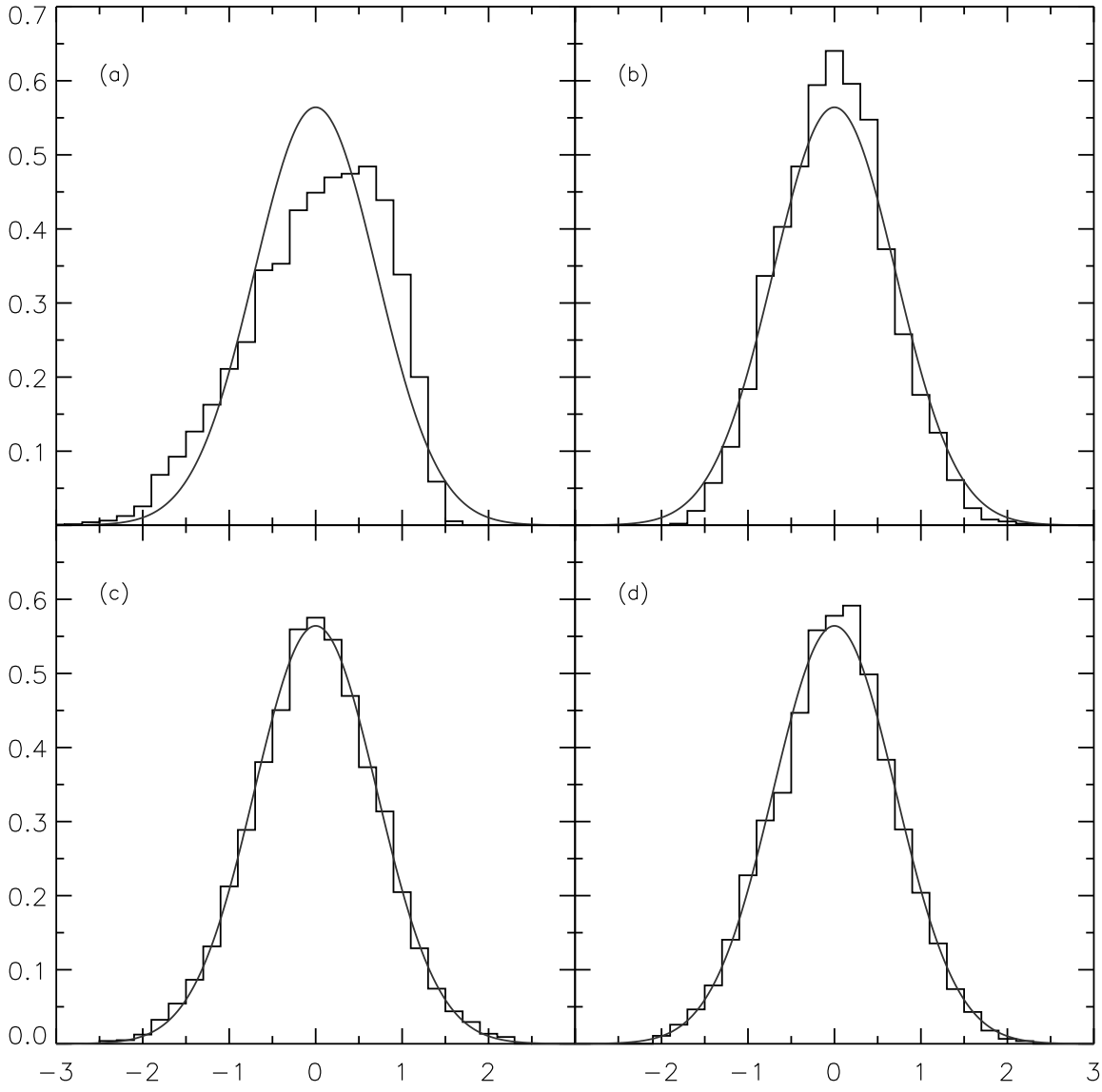

Fig. 4

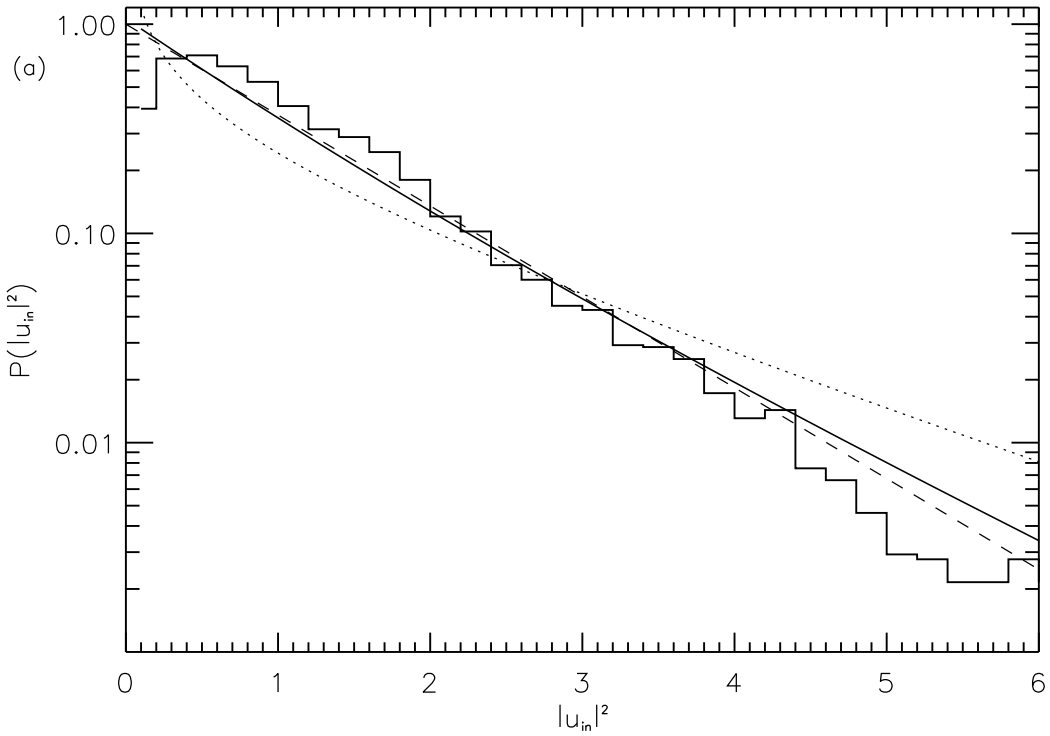
(a)
1.00
0.10
0.01
P(|u_in|²)
0
1
2
3
4
5
6
|u_in|²

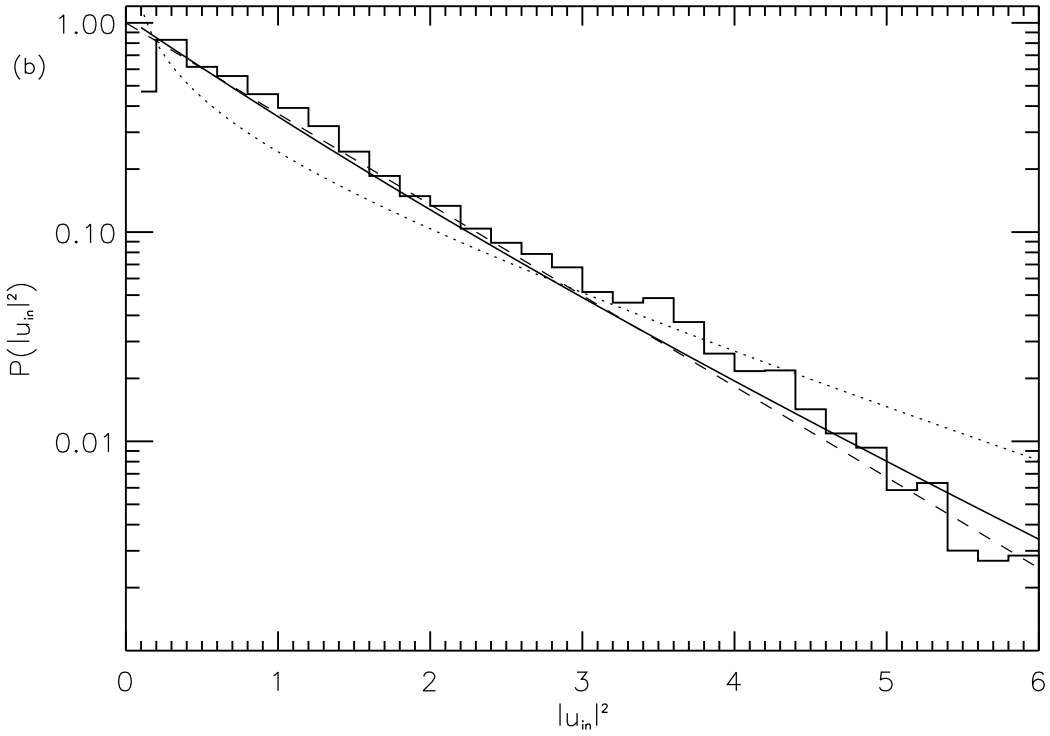
(b)
1.00
0.10
0.01
P(|u_in|²)
0
1
2
3
4
5
6
|u_in|²

Fig. 5